

## Medial Plate for Treatment of Distal Tibia Fractures

G. Theisz<sup>1,2,\*</sup>, K. Frydryšek<sup>1,2</sup>, F. Fojtík<sup>1,2</sup>, T. Kubín<sup>1,3</sup>, L. Pečenka<sup>1,5</sup>, J. Demel<sup>6</sup>,  
R. Madeja<sup>6</sup>, M. Sadílek<sup>1,4</sup>, J. Kratochvíl<sup>1,4</sup>, L. Pleva<sup>6</sup>

<sup>1</sup> VSB–Technical University of Ostrava, Faculty of Mechanical Engineering, 17. listopadu 15/2172,  
708 33 Ostrava, Czech Republic

<sup>2</sup> Department of Applied Mechanics

<sup>3</sup> Department of Production Machines and Design

<sup>4</sup> Department of Machining and Assembly

<sup>5</sup> Department of Applied Mechanics, IT4Innovations Centre of Excellence

<sup>6</sup> Ostrava University Hospital, Trauma Centre, 17. listopadu 1790, 708 52 Ostrava, Czech Republic  
& University of Ostrava, Faculty of Medicine, Dvořákova 7, 701 03 Ostrava, Czech Republic

\* gunther.theisz@vsb.cz

**Abstract:** The objective of the present study was to carry out a strength and reliability assessment of a medial plate for the treatment of distal tibia fractures. This was performed via numerical modelling (FEM) and experimental methods (compression test and Electronic Speckle Pattern Interferometry – ESPI method). The plate is used for internal fixation in orthopaedics and traumatology. Analyses were performed for non-fused bone with comminuted fracture in the distal metaphysis (i.e. unsuccessful treatment, where all loads in the metaphysis are carried by the plate). An anatomical tibia model (based on CT images in Mimics software) was used for FE analysis. In the experiments, the bone was replaced with a shaped piece of spruce wood (based on Mimics software) and the plate was loaded until its failure (major plastic deformation). Numerical and experimental results were evaluated and compared.

**Keywords:** Medial Plate; Tibia; Biomechanics; FEM; Compression Test; ESPI Method; Failure; Traumatology; Orthopaedics; Strength Analysis.

## 1 Introduction

Medial plates are internal fixators (implants). They are used for the purpose of fixation and stabilization of bone in traumatology and orthopaedics; see Fig. 1. Successful treatment also depends on the reliability of implants. In the case of failure (i.e. unsuccessful treatment), it is necessary to perform osteosynthesis again. Unfortunately, no type of treatment can achieve 100 percent success rates. The situation of maximum loading on non-fused bone is an extreme state in which the fracture fails to heal (i.e. with loading even exceeding yield stress and the patient is not permitted to walk).

## 2 FE Analysis

The FE analysis (i.e. calculation of stresses and total displacements) was performed with an anatomical tibia model based on CT images in MSC Patran software. The described material properties of bone correspond with partially non-homogeneous isotropic material models (elastic modulus and Poisson's ratio for each element of the tibia); see Fig. 2. The calculation of bone tissue density is carried out using Mimics software on the basis of greyscale values (GV), which are derived from the Hounsfield unit (HU). The Mimics software manual gives the relation between the calculation of GV and HU; see Eq. (1). Density in a given element is then calculated according to Eq. (2). The resulting elastic modulus is gained for individual elements from this density; see Eq. (3). These equations and the constants within them are valid for typical bone tissue. Poisson's ratio is

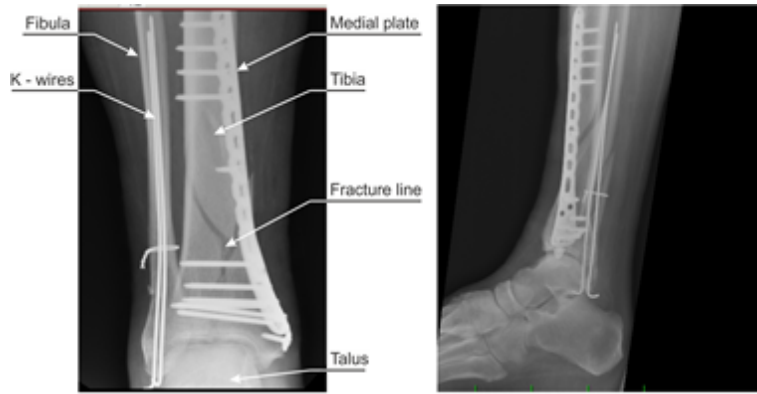


Fig. 1: X-ray snapshots after fixation with plate.

identical for all elements;  $\mu = 0.3$ . An extensive summary of 18 studies and 22 equations of relations between the elastic modulus and HU is described in the literature [1]. Other relations between the elastic modulus and bone tissue density are described in [2–4].

$$GV_{(x,y,z)} = HU_{(x,y,z)} + 1024 \quad [-] \quad (1)$$

$$\rho_{(x,y,z)} = -13.4 + 1017 \cdot GV_{(x,y,z)} \quad [\text{g} \cdot \text{m}^{-3}] \quad (2)$$

$$E_{(x,y,z)} = -388.5 + 5925 \cdot \rho_{(x,y,z)} \quad [\text{Pa}] \quad (3)$$

The description of the material behaviour of the bone was based on a total of 100 different elastic moduli calculated on the basis of HU for individual elements. In the diaphysis area the value of the elasticity modulus of the cortical tissue is maximal (16874.03 MPa) and the value of the spongiosal tissue is minimal (5081.5 MPa); this corresponds with reality.

The precise determination of tibia loading is a complex problem, and so loading is defined as follows. When standing on one limb, with the other limb slightly raised and bent, the tibia is loaded by compression along its axis. The unitary loading  $F = 1 \text{ N}$  was selected for the analysis. Unitary loading is practical for linear solutions because the results are easy to convert to real loading in the elastic area (the resulting stress and deformation need only to be multiplied by the actual value of the force). Unitary force  $F$  acts in the positive direction of axis  $Z$  in coordinate system 1; see Fig. 3. Using the multi-point constraint, force was applied to the cross-section of the cortical tissue in the transverse plane in the vicinity of the proximal metaphysis. The location of this force was selected based on the position of the knee joint in CT scan images.

The unitary force  $F$  was applied to the same surface; a boundary condition was prescribed in order to substitute for the knee joint ( $X = Y = 0$  for coordinate system 1); see Fig. 3. The ankle joint was substituted by a boundary condition restricting movement along all three axes  $X = Y = Z = 0$  for coordinate system 2); see Fig. 3. The size of the surface to which this boundary condition was applied corresponds with the contact surface between the tibia and the talus.

The FE model contains 185 094 nodes and 1 015 155 elements. The geometry of the screws is simplified by substituting the thread with a cylindrical surface. Likewise, the lockable screw threads in the plate are substituted by conical surfaces. A fixed glue-type contact joint is defined between the screws and the tibia, and between the screws and the plate.

The course of the movement in a medial plate made of AISI 316L steel, loaded with unitary force, is shown in Fig. 4 (maximum  $2.2 \times 10^{-2} \text{ mm}$ ). The distribution of the reduced stress according to the HMM hypothesis (maximum 1.82 MPa for unitary force) is shown in Fig. 5. The maximum calculated stress is at the position of the oval hole and at the position of the hole for the angularly stable screw. This represents an extreme case in which the patient is not permitted to walk and the bone is not fused at all; the loading is transferred solely by the plate (unsuccessful treatment).

The ESPI is then used to examine and compare the oval hole.

The mechanical properties of the AISI 316L steel used to make the plate and the lockable screws were determined via a tensile test. The results of the test are given in Tab. ??.

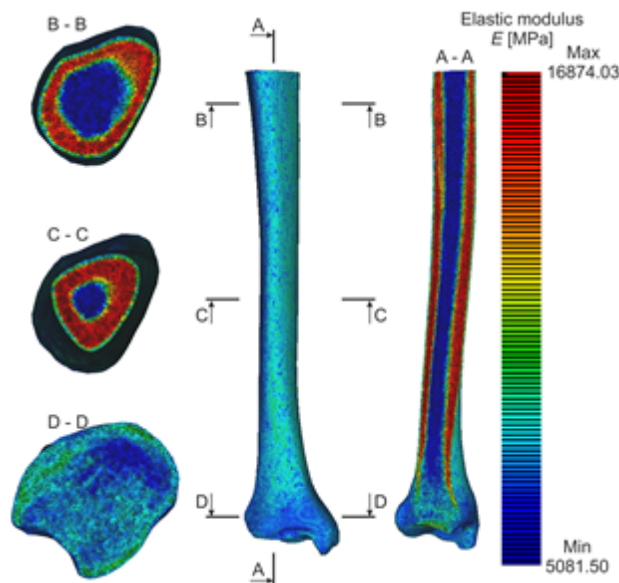


Fig. 2: Size of elasticity modulus.



Fig. 3: Substitution of knee and ankle joint.

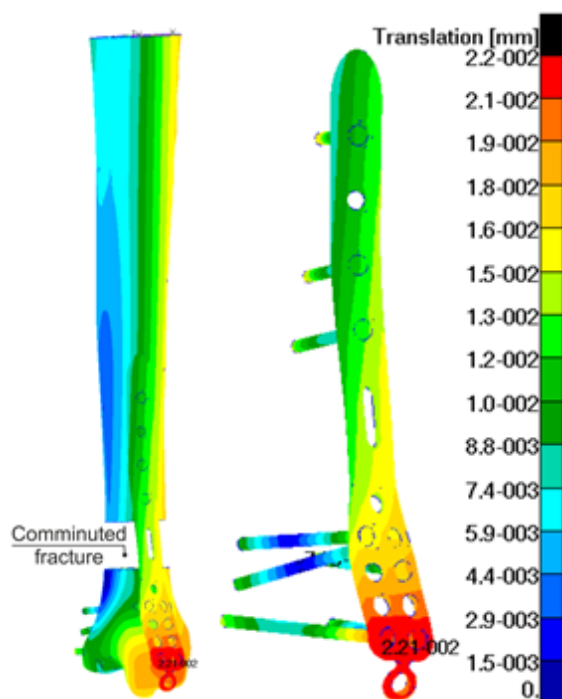


Fig. 4: Course of movement (AISI 316L steel, non-fused bone, force  $F = 1$  N).

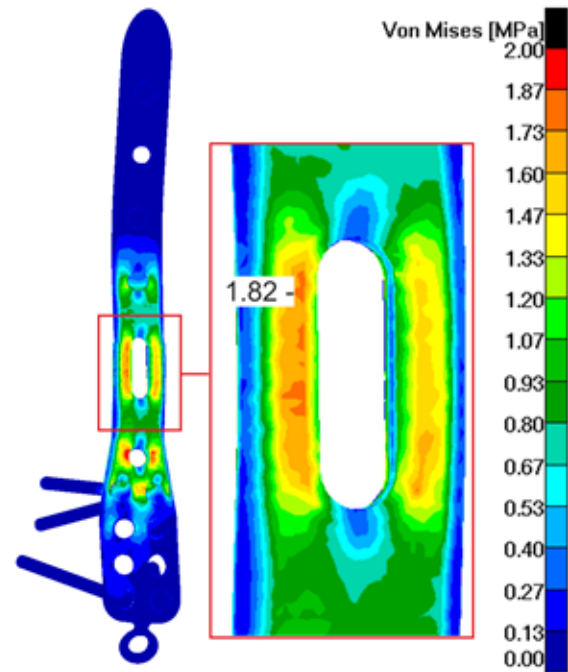


Fig. 5: Reduced stress according to HMH hypothesis (AISI 316L steel, non-fused bone, force  $F = 1$  N).

Tab. 1: Results for mechanical properties determined via tensile testing for AISI 316L steel.

Samples	$E$ [GPa]	$R_{p0,2}$ [MPa]	$R_m$ [MPa]
Sample 1	212	904	979
Sample 2	209	887	972
Sample 3	208	885	980
Mean value	209.7	892	977

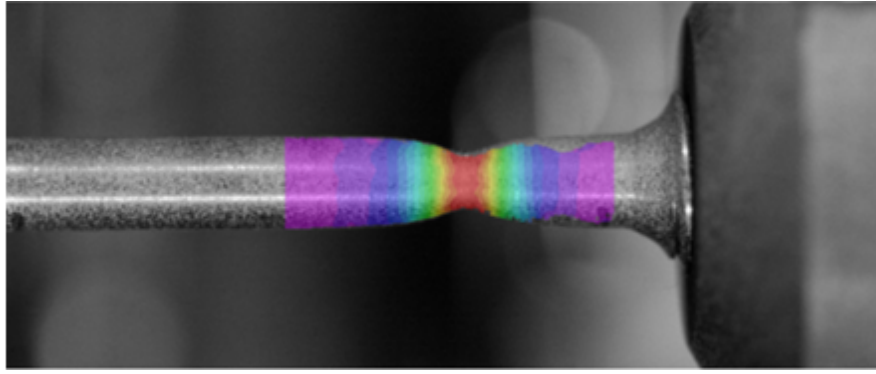


Fig. 6: Tensile test (sample AISI 316L) – distribution of strain fields determined by DIC.

Tab. 2: Maximum permissible loading  $F_{max}$  (AISI 316L steel).

Material	AISI 316L steel
Material yield stress $\sigma_y$ [MPa]	892
Maximum calculated stress according to HMM theory $\sigma_{max}$ [MPa] at $F = 1$ N	1.82
Maximum permissible loading $F_{max}$ [N] (at yield stress)	490.11

The analysis of the plate was performed in the area of elasticity, so it is possible to calculate the maximum permissible loading  $F_{max}$  with regard to the yield stress as the ratio of yield stress  $R_{p0.2}$  and the maximum calculated stress  $\sigma_{max}$ . The maximum permissible loading for a medial plate made of AISI 316L steel is 490.11 N; see Tab. 2 (this corresponds with a static loading of 49.98 kg when standing on one leg). This represents an extreme case in which the entire loading in the area of the metaphysis is transferred by the plate (i.e. unsuccessful treatment, in which the bone does not fuse and the patient is not permitted to walk). In the case of successful treatment the value for permissible loading is many times higher, and the plate serves merely as a support structure because the bone is fully fused.

### 3 Experiments

#### 3.1 Fixation of the Plate to a Jig

Experiments with implants are described e.g. in [3]. For such experiments a simple and cheap recommended solution involves replacing the tibia bone with an anatomically shaped testing jig made from spruce wood. Our first experiments with beech wood were problematic because the medical drilling machine lacked the necessary capacity. The plate for the “non-fused fracture” is attached to the wooden bone with the original bolts according to a surgical manual compiled by doctors from the University Hospital of Ostrava; see Fig. 6.

In order to achieve a more precise fixation of the plate, the distal and proximal part of the jig is fixed using manual clamps including a part which enables the plate to be fixed in an identical position for repeated experiments.

The plate is fixed to the testing jig according to the operating instructions given. The first fixation is performed by K-wires inserted into designated holes or using a guiding capsule. The plate is then fixed so it will not move during further fixation with angularly stable screws. Before applying these screws, a hole must be drilled using a special drill with a sleeve ensuring that the hole is drilled precisely in the correct direction. Each individual differs to some extent in their bone geometry. It is therefore not possible for the plate to match the precise shape of the bone in all cases. In order to ensure vascular supply to the bone tissue it is also important that the plate should not be in full direct contact with the bone.

This factor is simulated by the K-wire, which creates a gap between the plate and the testing jig in its proximal part. In the distal part this gap is eliminated as far as possible. The screws are tightened using a special torque screwdriver set to a value of 1.5 Nm. In the proximal part there are 3 lockable screws. One hole is left empty in order to achieve maximum stress distribution. There are a total of 5 screws in the distal part. Again some holes are left empty to achieve better stress distribution, as is standard operating practice.

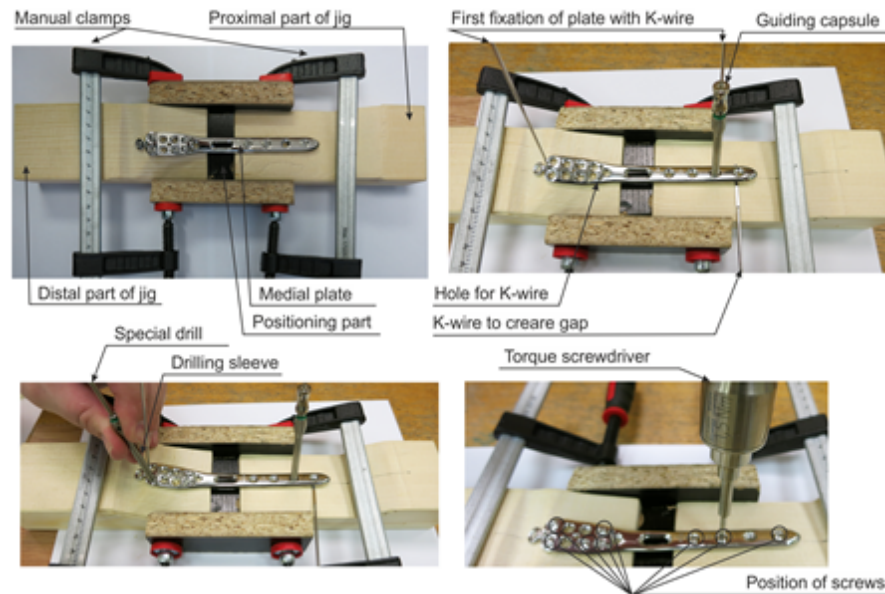


Fig. 7: Fixation of the plate to the testing jig.

### 3.2 The ESPI Method

Optical non-destructive experimental methods are currently becoming increasingly widespread. The company Dantec-Dynamics has market-launched its newly designed Q-100 system including a laser optical sensor for quantitative measurement of stress deformation.

The ESPI method (Q-100 sensor) was applied to problems of elasticity in order to determine the contours of bending stress at the oval hole; see Fig. 7. Standard material parameters (Young's modulus  $E = 209.7$  MPa and the Poisson number  $\mu = 0.3$ ) can also be used to determine stress distribution in the area of measurement according to the HMM hypothesis; see Fig. 8. As the testing jig represents a difference compared with the FE analysis, the course of the stress is also different. For the FEM analysis the plate was loaded mainly for bending, while in the experiment combined loading occurs due to the geometry and fixation of the testing jig; this can be seen in Fig. 8. The maximum stress at loading  $F = 140$  N is 282.2 MPa according to the HMM hypothesis (corresponding with a stress of 2.01 MPa for unitary loading).

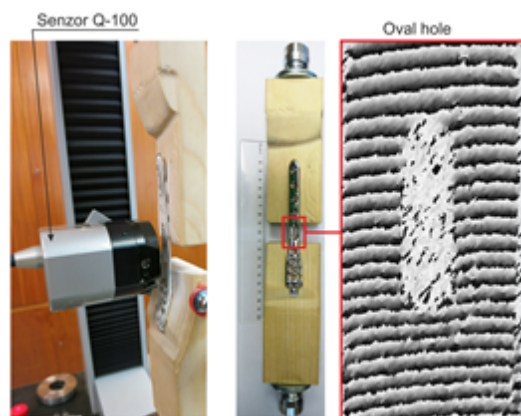


Fig. 8: Wooden preparation and ESPI fringers around oval hole of plate.

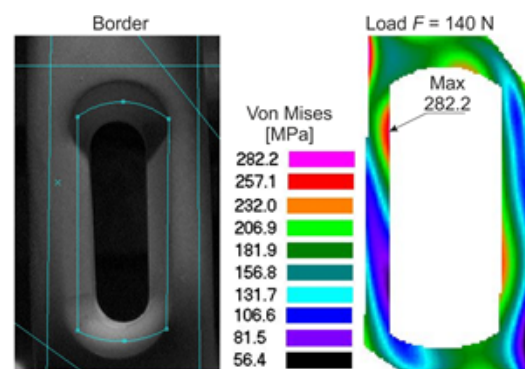


Fig. 9: Border of results and course of bending stress according to HMM hypothesis [MPa].

### 3.3 Compression Test (Overload of Plate)

A compression test was applied to the entire elastic-plastic region; see Fig. 9. (i.e. dependence of axial force on axial displacement, overloading caused mostly by compression and bending, buckling, large deformations and failure are evident). The maximum permissible loading is set according to the compression test diagram as



Tab. 3: Comparison of maximum permissible loading of plate.

	Maximum permissible loading $F_{max}$ [MPa]	Difference [%]
Experiment (compression test)	525	-
Experiment (ESPI method)	443.78	15.47
Finite Element Method	490.11	6.64

525 N. The experiment was performed on a TENSOMETRIC M500 – 50 CT; see Fig. 10. The testing jig was loaded to the point of complete destruction; see Fig. 9.

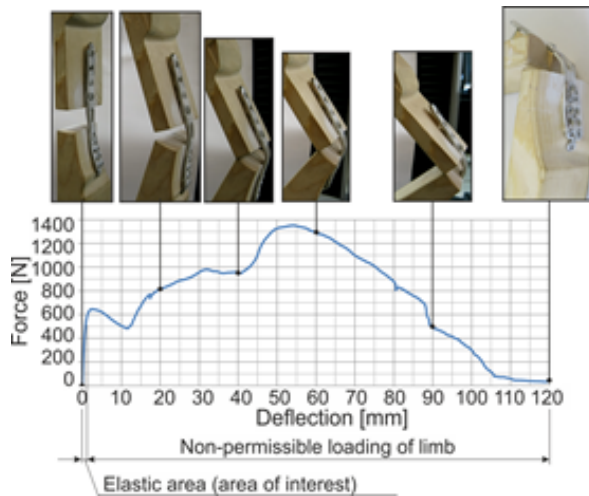


Fig. 10: Dependence of axial force on axial deflection.



Fig. 11: Tensometric M500 – 50 CT with plate.

## 4 Comparison of Results

A comparison of the results in the elastic region from the FE analysis and the experiment is shown in Tab. 3. The maximum permissible loading according to the ESPI method differs from the compression test by 15.47 %. The difference between the compression test and FE analysis is 6.64 %. In view of the real differences between the experiment (the plate fixed to a wooden jig) and the FE model with a real bone, the results are acceptable.

## 5 Conclusion

This paper analyzes medial plates for osteosynthesis of distal tibia (producer Medin, a.s.). It presents FE modelling and measurements (compression tests and ESPI method) for non-fused bone (i.e. extreme situations connected with failure and unsuccessful treatment, when walking is not permitted). Comparison experiments with numerical calculations provide a higher degree of certainty in verifying the reliability of the plate. In the case of unsuccessful treatment, when the bone does not fuse and the plate transfers the entire loading, it is necessary to perform the operation again. In the case of successful treatment, the value for permissible loading is many times higher, and the plate serves merely as a support structure; it can thus be considered safe.

It should be mentioned that the results are not relevant for conclusions regarding the dynamic strength of the product. To determine relevant results for dynamic strength it would be necessary to perform an extensive and costly experiment defining the dependency of the number of cycles and loading force. Nevertheless, it has been proved that in the case of unsuccessful treatment, if the bone does not fuse, it is necessary to perform the operation again.

Future developments will involve the comparison of successful and unsuccessful treatments, the use of a plastic model in FEM analysis, and the cyclical loading of the plate to determine limit fatigue strength. Another possibility is the application of probability methods.

The authors gratefully acknowledge the funding from the Czech projects TA03010804, SP2015/180 and CZ.1.05/1.1.00/02.0070.

## References

- [1] B. Helgason et al., Mathematical Relationships between Bone Density and Mechanical Properties, *Clinical Biomechanics* (2008), 135-146, doi: [10.1016/j.clinbiomech.2007.08.024](https://doi.org/10.1016/j.clinbiomech.2007.08.024).
- [2] Cody, D. D. et al., Short term in vivo precision of proximal femoral finite element modeling. *ANNALS OF BIOMEDICAL ENGINEERING*. 2000, vol. 28, č. 4, s. 408-414.
- [3] Keyak, J. H. a Y. Falkinstein. Comparison of in situ and in vitro CT scan-based finite element model predictions of proximal femoral fracture load. *Medical Engineering and Physics*. 2003, vol. 25, č. 9, 781 – 787, doi: [10.1016/S1350-4533\(03\)00081-X](https://doi.org/10.1016/S1350-4533(03)00081-X).
- [4] Morgan, Elise F., Harun H. Bayraktar a Tony M. Keaveny. Trabecular bone modulus–density relationships depend on anatomic site. *Journal of Biomechanics*. 2003, roč. 36, č. 7, s. 897-904. doi: [10.1016/S0021-9290\(03\)00071-X](https://doi.org/10.1016/S0021-9290(03)00071-X).
- [5] K. Frydrýšek et al., About the Verification of External Fixators Applied in Traumatology and Orthopaedics, 52nd International Conference on Experimental Stress Analysis (2014), 153-160, doi: [10.4028/www.scientific.net/AMM.732.153](https://doi.org/10.4028/www.scientific.net/AMM.732.153).
- [6] K. Frydrýšek et al., Design of External Fixators used in Traumatology and Orthopaedics – Treatment of Fractures of Pelvis and its Acetabulum, *Procedia Engineering* (2012), 164-173, doi: [10.1016/j.proeng.2012.09.501](https://doi.org/10.1016/j.proeng.2012.09.501).
- [7] K. Frydrýšek et al., New Ways for Designing External Fixators Applied in Treatment of Open and Unstable Fractures. *World Academy of Science* (2011), 697 – 702.
- [8] Vilimek, Miloslav, a R. Sedláček. 2011. Methodology for Dynamic Testing of Plates for Proximal Tibia Osteosynthesis. *Bulletin of Applied Mechanics*. 7(25): 12-14. ISSN 18011217.